Highly dispersive coupled modes in a SiN/SiO_2/Si heterostructure

Md Borhan Mia and Sangsik Kim*

Department of Electrical and Computer Engineering, Texas Tech University, Lubbock, Texas 79409, USA

**sangsik.kim@ttu.edu*

Abstract: We present a SiN/SiO_2/Si heterostructure that can achieve extremely high dispersions ($>|\pm 10^7|$ ps$\cdot$nm^{-1}km^{-1}). The large group velocity difference between the SiN and Si waveguides results in such high dispersions.

OCIS codes: (130.0130) Integrated optics, (230.7370) Waveguides, (260.2030) Dispersion

Dispersive photonic components that control the dispersion of a system play a vital role in ultrafast signal processing, since they determine the chirp rate and duration of an optical signal. To control the dispersion of a system, different types of on-chip photonic structures have been proposed, for example, coupled strip-slot [1] or asymmetric slot [2] waveguides and concentric microresonators [3]. In these structures, a mode coupling phenomenon was utilized to control the dispersion; i.e., when two asymmetric modes are in close proximity and coupled, the coupled symmetric/anti-symmetric modes are associated with normal/anomalous dispersions. Here, we present a heterogeneously coupled SiN/SiO_2/Si waveguide structure, the asymmetric modes of which are given by silicon nitride (SiN) and silicon (Si) waveguides. The large group velocity difference between the waveguide modes of Si and SiN results in such extremely high dispersions, and we achieve more than ten million ($>|\pm 10^7|$) ps$\cdot$nm^{-1}km^{-1} at the dispersion peaks.

Figure 1(a) shows the schematic view of the proposed waveguide, which is stacked with the Si (red), SiO_2 (grey), and SiN (blue) layers. The thickness of the Si, SiO_2 and SiN layers are h_1, h_2, and h_3, respectively, and every layer shares the same width w_0. Such SiN/SiO_2/Si multilayer structures can be fabricated through the integration of SiN on top of a silicon-on-insulator (SOI) wafer or through the post-bonding process of the two separate (SOI and SiN) wafers. Figure 1(b) shows the simulated effective indices n_{eff} of the coupled symmetric (solid orange line) and anti-symmetric (solid blue line) supermodes. The orange and blue dashed lines are the n_{eff} of the isolated fundamental TM (TM_0) modes of Si and SiN waveguides, respectively. Notice that there is a bending in n_{eff} of the symmetric and anti-symmetric modes near the wavelength $\approx$ 1552.8 nm, where the n_{eff} of the two isolated TM_0 modes (dashed orange and blue lines) crosses and the mode coupling occurs. The inset figures are the modal field distribution of each mode at different wavelengths and show the mode transition through the mode coupling. The bending effect in n_{eff} of the coupled modes induces normal and anomalous dispersions to the symmetric and anti-symmetric modes, respectively. Figure 1(c) is the dispersion profiles of the coupled modes (orange line: symmetric mode, blue line: anti-symmetric mode) that are calculated using n_{eff} data of Fig. 1(b) ($D_\lambda = -\frac{\lambda}{c}\frac{\partial^2 n_{\text{eff}}}{\partial \lambda^2}$). This figure clearly shows the induced anomalous/normal dispersions to the anti-symmetric/symmetric modes.

The peak values ($D^{\pm}_{\lambda,\max}$) and the bandwidth ($\delta\lambda$) of dispersions can be represented as the following [4],

$$D^{\pm}_{\lambda,\max} = -\frac{\lambda^2}{4\pi c}\left(D_{\lambda_1}+D_{\lambda_2}\right) \mp \frac{1}{4|\kappa|}\left(\frac{1}{v_1}-\frac{1}{v_2}\right)^2 \tag{1}$$

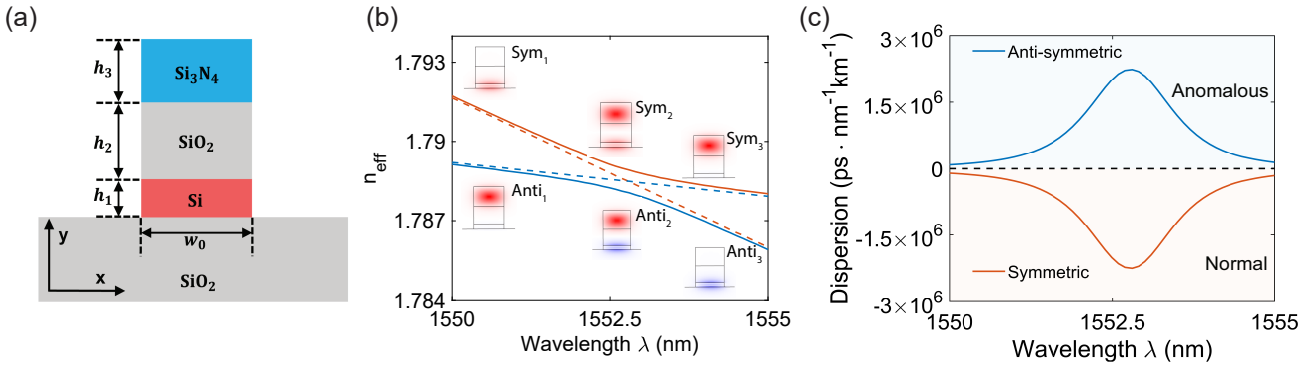

Fig. 1: (a) Schematic view of the coupled SiN/SiO_2/Si waveguide structure with geometric parameters: heights of the Si (h_1), SiO_2 (h_2), and SiN (h_3) layers and widths of them w_0. (b) Simulated effective indices (n_{eff}) of the coupled symmetric (Sym, solid orange line) and anti-symmetric (Anti, solid blue line) modes, respectively. Orange and blue dashed lines are the n_{eff} of the isolated fundamental TM modes of Si and SiN waveguides, respectively. Inset figures show the field distribution of each coupled mode at corresponding wavelengths. (c) Dispersion profiles of symmetric (orange) and anti-symmetric (blue) modes that correspond to the (b). The geometric parameters are $h_1 = 200$ nm, $h_2 = 1200$ nm, $h_3 = 1050$ nm, and $w_0 = 1000$ nm.

978-1-7281-0615-1/19/$31.00 ©2019 IEEE

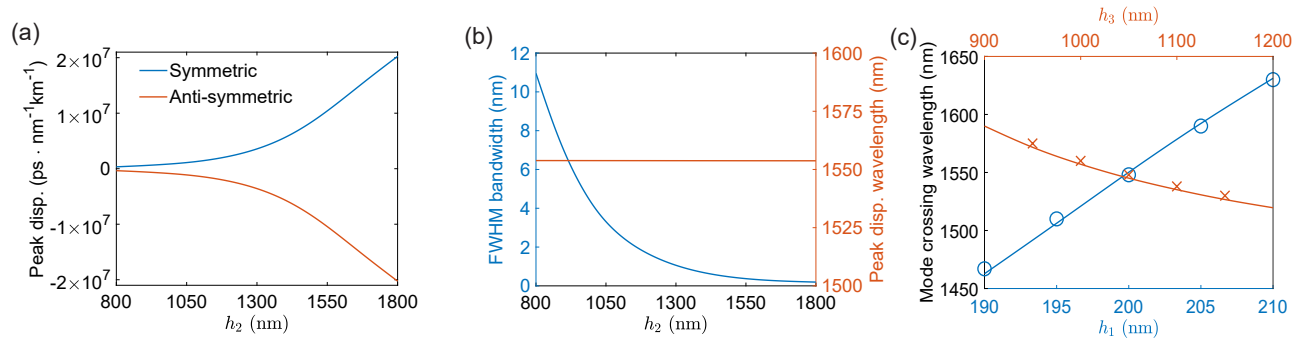

Fig. 2: (a) Simulated dispersion peaks (blue: anti-symmetric, orange: symmetric) as a function of SiO_2 spacer thickness h_2. (b) The full-width-half-maximum (FWHM) bandwidth (blue) and the peak dispersion wavelengths (orange) that correspond to the (a) (as a function of h_2). Other parameters are the same as in Fig. 1. (c) Mode crossing wavelength of the isolated SiN and Si waveguides as a function of h_1 (blue line, fixing the $h_3 = 1050$ nm) and h_3 (orange line, fixing the $h_1 = 200$ nm). The other parameters are $h_2 = 1500$ nm and $w_0 = 1000$ nm. Blue circles and orange crosses represent the corresponding peak dispersion wavelengths of the coupled modes from the full modal simulations.

$$\delta\lambda = 2|\kappa|\left|\frac{1}{v_1} - \frac{1}{v_2}\right|^{-1} \tag{2}$$

where v_i and D_{λ_i} are the group velocity and dispersion of the isolated mode without a coupling ($i = 1, 2$), and κ is the coupling coefficient between the two isolated modes. The $D^{+}_{\lambda,\max}$ and $D^{-}_{\lambda,\max}$ indicate symmetric and anti-symmetric modes, respectively. Equation 1 indicates that the peak values of the dispersions ($D^{\pm}_{\lambda,\max}$) are quadratically proportional to the group velocity difference and inversely proportional to the coupling coefficient κ between the two isolated modes. In our configuration, the large group velocity difference is introduced by using two different sets of materials (Si and SiN) for the waveguides; this is the main advantage of using the $Si/SiO_2/SiN$ coupled waveguide for achieving the extremely high dispersions. The coupling coefficient κ can be engineered to control the dispersion peaks and the bandwidth. The κ depends on the modal overlap between the two isolated modes; thus, changing the SiO_2 spacer thickness (h_2) will vary κ between two waveguides; i.e., increasing the h_2 reduces the κ that results in higher dispersion peaks (Eq. 1) and a narrower bandwidth (Eq. 2). It's the opposite for decreasing the h_2. To confirm these, we simulated the dispersion peaks and the bandwidths of the coupled modes for different h_2, and these results are plotted in Figs. 2(a) and 2(b), respectively. As suspected, the magnitudes of the dispersion peaks increase as the h_2 increases (Fig. 2(a)), and the peak dispersions can be higher than $|\pm 10^7|$ ps $\cdot$ nm^{-1}km^{-1} when $h_2 > 1500$ nm. On the other hand, the full-width-half-maximum (FWHM) bandwidth decreases as the h_2 increases (Fig. 2(b)). In general, there is a trade-off between the peak dispersion and the bandwidth, depending on the κ. This trade-off is clearly shown in Eqs. 1 and 2. The wavelength of the dispersions peaks is also plotted in Fig. 2(b) and it is almost identical at ≈ 1553 nm, as changing the h_2 does not shift the mode crossing wavelength. To shift the wavelength of the dispersion peaks, the mode crossing wavelength needs to be shifted; and, this can be done by engineering the thickness of the Si (h_1) and SiN (h_3) layers. Figure 2(c) shows the shift of the mode coupling wavelengths as a function of h_1 (blue line, fixing the $h_3 = 1050$ nm) or h_3 (orange line, fixing the $h_1 = 200$ nm). The blue circles and orange crosses are the wavelengths of the dispersion peaks from the full simulations and they match well with the mode crossing wavelengths (solid lines). The degrees of shift are $\Delta\lambda_c/\Delta h_1 \approx 4.3$ nm/nm and $\Delta\lambda_c/\Delta h_3 \approx 0.68$ nm/nm; thus, we can use the h_1 and h_3 as coarse and fine tuning knobs, respectively, to control the mode coupling wavelength.

In summary, we proposed a heterogeneously coupled $SiN/SiO_2/Si$ waveguide structure for extremely high dispersions. The coupling strength between the SiN and Si waveguides can be engineered to control the dispersion peaks, and the large group velocity difference between the two waveguides allowed for such high dispersions ($> |\pm 10^7|$ ps $\cdot$ nm^{-1}km^{-1}). The wavelength of the dispersion peaks also can be engineered by changing the thickness of the Si and SiN layers, and this scheme should be useful in diverse applications of ultrafast signal processing and on-chip RF filters.

References

1. L. Zhang *et al.*, "Highly dispersive slot waveguides," Opt. Express **17**, 7095 (2009).
2. S. Kim and M. Qi, "Broadband second-harmonic phase-matching in dispersion engineered slot waveguides," Opt. Express **24**, 773 (2016).
3. S. Kim *et al.*, "Dispersion engineering and frequency comb generation in thin silicon nitride concentric microresonators," Nat. Commun. **8**, 372 (2017).
4. M. Mia, N. Jaidye, and S. Kim, "Extremely high dispersions in heterogeneously coupled waveguides," Opt. Express **27**, 10426 (2019).